AFRL-AFOSR-JP-TR-2018-0076

Nanostructured Array in Photocatalytic Device Design for Energy Applications

Tai-Chou Lee
NATIONAL CENTRAL UNIVERSITY
300, JHONGDA RD.
CHUNGLI CITY, 32001
TW

10/22/2018
Final Report

DISTRIBUTION A: Distribution approved for public release.

Air Force Research Laboratory
Air Force Office of Scientific Research
Asian Office of Aerospace Research and Development
Unit 45002, APO AP 96338-5002

REPORT DOCUMENTATION PAGE

Form Approved
OMB No. 0704-0188

The public reporting burden for this collection of information is estimated to average 1 hour per response, including the time for reviewing instructions, searching existing data sources, gathering and maintaining the data needed, and completing and reviewing the collection of information. Send comments regarding this burden estimate or any other aspect of this collection of information, including suggestions for reducing the burden, to Department of Defense, Executive Services, Directorate (0704-0188). Respondents should be aware that notwithstanding any other provision of law, no person shall be subject to any penalty for failing to comply with a collection of information if it does not display a currently valid OMB control number.
PLEASE DO NOT RETURN YOUR FORM TO THE ABOVE ORGANIZATION.

1. REPORT DATE *(DD-MM-YYYY)*	2. REPORT TYPE	3. DATES COVERED *(From - To)*
22-10-2018	Final	21 Jul 2017 to 20 Jul 2018

4. TITLE AND SUBTITLE
Nanostructured Array in Photocatalytic Device Design for Energy Applications

5a. CONTRACT NUMBER

5b. GRANT NUMBER
FA2386-17-1-4028

5c. PROGRAM ELEMENT NUMBER
61102F

6. AUTHOR(S)
Tai-Chou Lee

5d. PROJECT NUMBER

5e. TASK NUMBER

5f. WORK UNIT NUMBER

7. PERFORMING ORGANIZATION NAME(S) AND ADDRESS(ES)
NATIONAL CENTRAL UNIVERSITY
300, JHONGDA RD.
CHUNGLI CITY, 32001 TW

8. PERFORMING ORGANIZATION REPORT NUMBER

9. SPONSORING/MONITORING AGENCY NAME(S) AND ADDRESS(ES)
AOARD
UNIT 45002
APO AP 96338-5002

10. SPONSOR/MONITOR'S ACRONYM(S)
AFRL/AFOSR IOA

11. SPONSOR/MONITOR'S REPORT NUMBER(S)
AFRL-AFOSR-JP-TR-2018-0076

12. DISTRIBUTION/AVAILABILITY STATEMENT
A DISTRIBUTION UNLIMITED: PB Public Release

13. SUPPLEMENTARY NOTES

14. ABSTRACT
The PI was successful in achieving their proposed objectives. They were able to preparing SiO2 core-metal sulfide shell nanoparticles with tunable thickness and focused their work on better coverage and crystallinity of SiO2@metal sulfide nanoparticles for future SPR studies and hydrogen production. In this work ZIS was used as the model photocatalyst. ZIS shells were synthesized using different solvents and results showed that ZIS synthesized in water exhibits a better crystallinity and a higher hydrogen production. As the results, we found the highest hydrogen generation efficiency was measured at 240 C synthesis. The PI is currently working on submitting publications in peer reviewed journals.

15. SUBJECT TERMS
Hydrogen Generation, Metal Nanoshells, Photocatalysis, Biomass Conversion, Hydrogen Generation, Core/Shell Nanoparticles, Dielectric Interlayers, Oxidation

16. SECURITY CLASSIFICATION OF:			17. LIMITATION OF ABSTRACT	18. NUMBER OF PAGES	19a. NAME OF RESPONSIBLE PERSON
a. REPORT	b. ABSTRACT	c. THIS PAGE			CHEN, JERMONT
Unclassified	Unclassified	Unclassified	SAR		19b. TELEPHONE NUMBER *(Include area code)* 315-227-7007

Standard Form 298 (Rev. 8/98)
Prescribed by ANSI Std. Z39.18

Final Report for AOARD Grant FA2386-17-1-4028 "Nanostructured Array in Photocatalytic Device Design for Energy Applications"

Date: Oct. 18, 2018

PI and Co-PI information:
PI: Tai-Chou Lee; taichoulee@ncu.edu.tw; National Central University; Department of Chemical and Materials Engineering; 300 Jhongda Road, Jhongli District, Taoyuan County, Taiwan; +886-3-4227151#34211

Co-PI: T. Randall Lee, trlee@uh.edu; University of Houston; Department of Chemistry; 4800 Calhoun Road, Houston, Texas 77204, United States; +1-713-7432724

Period of Performance: Jul. 21, 2017 to Jul. 20, 2018

Abstract

$ZnIn_2S_4$ (ZIS) is a visible-light-driven photocatalyst with energy band gap of 2.4 eV. In our previous work, we developed a microwave-assisted hydrothermal method to generate ZIS particles. The gold-silver nanoshells (GS-NS) with tunable absorption were embedded in ZIS matrix for plasmonic-enhanced photocatalytic hydrogen production. However, the coverage and thickness of ZIS on GS-NS were not precisely controlled. If the crystallinity and coverage of ZIS can be improved and the ZIS shell thickness can be tuned, we can find out the key factors that affect hydrogen production efficiency. In this work, we specifically focused on improving the coverage and crystallinity of ZIS shells synthesized using microwave-assisted hydrothermal method by pH control in ethanol. The modification on SiO_2 nanoparticle surfaces was also critical to generate a homogeneous ZIS coverage. The results showed that SiO_2@ZIS has the better coverage and crystallinity synthesized in the ethanol solution under a lower pH condition with surface modification. Thickness of ZIS shell could easily be controlled by adding different concentration of ZIS precursor. SiO_2@ZIS synthesized in ethanol at pH 1 showed the best coverage and crystallinity, perhaps due to the faster decomposition rate of thioacetamide in ethanol. In a parallel experiment, $AgInS_2$-ZnS solid solutions (AIZS) were deposited onto the SiO_2 surface. AIZS is known for its controllable band gap (from 1.8 to 3.6 eV) by changing the chemical compositions. The effects of different synthesis temperatures from 200 ˚C to 240 ˚C were investigated. Oleylamine and 1-dodecanthiol were used as solvent and surfactants, respectively. The electrolyte for hydrogen production experiments was the mixture of 220 mL de-ionized water containing 0.35 M Na_2S and 0.25 M K_2SO_3. It was found that homogeneous AIZS nanoparticles were generated at a higher temperature, leading to a higher coverage on SiO_2 surface. Hydrogen evolution rate can reach 100 μmol/h*g when SiO_2@AIZS was synthesized at 240 ˚C.

DISTRIBUTION A: Approved for public release, distribution unlimited

Introduction

Energy has always been a key element for human civilization and development. It can be justified by the different forms of energies in stages of human evolution. In the twenty-first century, environmental problems are emerging and climate change issues are becoming more and more important. Of the current alternative energy sources, hydrogen is the most important because it is a clean source that converts sustainable solar energy to hydrogen, and only generates energy and water after using.[1-3] In contrast to metal oxides, the metal sulfides are potential materials as photocatalysts with suitable energy gap and visible-light activity.[4-7] For example, ternary sulfide $ZnIn_2S_4$, (ZIS) which is synthesized by a facile microwave hydrothermal method, is treated as an efficient visible-light-driven photocatalyst[8-10].

Unfortunately, most photocatalyst materials suffer from fast recombination kinetics, which decreases hydrogen production. Core-shell structure with surface plasmon resonance (SPR) properties can mitigate the problem. The SPR enhances the electric field close to the metal surface and absorb light.[22-24] In our previous work, we developed a facile strategy to generate ZIS particles on top of gold-silver nanoshells (GS-NS). The unique gold-silver nanoshells (GS-NS) with tunable absorption that were embedded in ZIS matrix demonstrated that the coupling between the SPR of the GS-NSs and the absorption of the ZIS photocatalyst were the key parameters to optimize solar hydrogen production.[17] However, the coverage and thickness of metal sulfide photocatalyst on GS-NS were not precisely controlled. In this work, we focused on preparing SiO_2 core-metal sulfide shell nanoparticles with tunable thickness of photocatalyst. We also focused on better coverage and crystallinity of SiO_2@metal sulfide nanoparticles for future SPR studies and hydrogen production.

In the first part of this research, ZIS was used as the model photocatalyst. ZIS shells were synthesized using different solvents. Some papers describ the synthesis of ZIS in different solutions, such as water, methanol and ethanol, etc.[25] The results showed that ZIS synthesized in water exhibits a better crystallinity and a higher hydrogen production. But none of these papers mentioned about the coverage of ZIS coating onto other materials. In our work, a better coverage of ZIS onto SiO_2 was obtained in ethanol. Unfortunately, the poor crystallinity limited the hydrogen production. In water, ZIS synthesized at lower pH would promote the crystallinity and hydrogen production.[26-28] pH control in ethanol is a facile and novel method to synthesize ZIS onto SiO_2. Separately, $AgInS_2$-ZnS (AIZS) solid solution was investigated. Since AIZS solid solution can easily tune the energy band gap, we attempt to prepare a series of photocatalyst shells with different absorptions. Using the hot injection method, various synthesis temperatures were employed in this research. We found that higher temperature could lead to more AIZS nanoparticles synthesizing and cause better coverage. As the results, we found the highest hydrogen generation efficiency was measured at 240 ˚C synthesis.

Experiments

Preparation of modified silicon dioxide (SiO_2) nanoparticles.

The preparation of silica followed the Stöber's method[29 30], 200 mL ethanol and 18 mL ammonium hydroxide were added to the round bottom flask under stirring for 5 min. 6.8 mL tetraethylorthosilicate was then added in the stock and maintain at 30 ℃. The mixture was further stirred overnight. In order to modify the surface of SiO_2 nanoparticles, 250 μL 3-mercaptopropyl

DISTRIBUTION A: Approved for public release, distribution unlimited

trimethoxysilane (MPS) was added into the mixture and stirred at 30 ℃ for 6 hr. Finally, the solution was refluxed at 88 ℃ for 1 hr. The mixture was then centrifuged at 2500 rpm for 1 hr to remove excess MPS. The precipitates were collected and re-dispersed into 50 mL absolute ethanol. The modified SiO_2 particles were dried in the oven, the weight of the particles was measured, and ethanol was added to prepare SiO_2 solution with fixed particle concentration (0.1 g SiO_2@MPS in 5 mL ethanol solution).

Preparation of SiO_2@MPS@ZIS composite structure.

In preparing bare ZIS particles, zinc nitrate hexahydrate (0.3 mmol), Indium (III) nitrate hydrate (0.6 mmol), and thioacetamide (2.4 mmol) were dissolved in 15 mL de-ionized (DI) water or absolute ethanol solution under vigorous stirring for 10 min. The solution was then poured into a 30 mL quartz vial. The hydrothermal reaction took place in a microwave reactor (Monowave 300, Anton Paar) at 120 ℃ for 10 min. The precipitates were collected and centrifuged at 8000 rpm for 10 min. The resulting particles were rinsed thoroughly with DI water several times, and they were then dried in an oven at 80 ℃ for 12 h. For the synthesis of SiO_2@MPS@ZIS nanoparticles, 5mL SiO_2@MPS in ethanol was re-dispersed in 10 ml ethanol solution using ultrasonic vibration. If synthesized in water is needed, dried 5 ml SiO_2@MPS ethanol solution (0.1 g SiO_2@MPS) was added 15 ml water. Zinc nitrate hexahydrate (0.3 mmol) and Indium (III) nitrate hydrate (0.6 mmol) were dissolved under a vigorous stirring for 10 min, which was then added with thioacetamide (2.4 mmol) and stirred 2 min. Certain amount of HCl into solution was added if pH control is needed. The reaction was carried out in a microwave oven at 120 ℃ for 10 min. The as-prepared SiO_2@MPS@ZIS particles were collected by centrifugation and washed with DI water several times. Finally, the composite particles were placed in an oven at 80 ℃ for 12 hours to remove excess water.

Preparation of SiO_2@MPS@AIZS core-shell nanostructure.

0.03 g SiO_2@MPS was added into a two-neck flask. Silver acetate (0.25 mmol), zinc acetate (0.5 mmol), indium acetate (0.25 mmol) and thiourea (1 mmol) were then pour into the flask. Oleylamine (OLA) and 1-dodecanethiol (DDT) were added into the stock as the solvent and surfactant, respectively. The solution was stirred until all precursors were dissolved. The solution was heated from 200 ℃ to 240 ℃ for 10 min. The SiO_2@MPS@AIZS nanoparticles were collected by centrifugation and washed by toluene, isopropanol for one time and methanol for several times. Finally, powders were placed into an oven at 80 ℃ for 12h to remove excess solvent.

Photocatalytic Hydrogen Evolution

The photocatalytic reaction of hydrogen production was carried out in a 300 mL custom-built two-neck cylindrical glass cell with a quartz side window. The illumination area is 27.733 cm^2. The sacrificial agent was prepared by adding potassium sulfite (0.25 mol/L) and sodium sulfide (0.35 mol/L) in 220 mL DI water. 0.03 g of prepared ZIS or SiO_2@MPS@ZIS particles were dispersed in the sacrificial solution and 1 wt% dihydrogen hexachloroplatinate (IV) hexahydrate was then added. The reactor was then connected to cold traps to prevent steam from coming into the GC

DISTRIBUTION A: Approved for public release, distribution unlimited

column. The system was operated at low pressure with gas circulation pump. Finally, the photocatalytic reactor was irradiated by a 300 W Xe lamp. The intensity was set at 100 mW/cm^2 (measured by an optical meter (Newport 1918-R)). The temperature was kept at 25 ℃ during the reaction and hydrogen gas was collected with online GC system. The evolved gas was analyzed using a China 8700F gas chromatography.

Characterizations.

Extinction spectra were obtained using a UV-visible Spectrophotometer (Jasco V-670) over the wavelength from 400 to 700 nm. Nanoparticles were dispersed in DI water or ethanol and measured using Dynamic Light Scattering (Malvern Nano-ZS9). Crystal structures were measured using an X-Ray Diffractometer (Brucker KAAPA APEX II). Cu Kα light source was used, in coupled with Ni filter. The scan rate was set at 3 °/min in the range of 10-80°. Transmission Electron Microscope (TEM; JEOL-JEM2000) and high resolution Transmission Electron Microscope (HRTEM; JEOL-JEM2100) were used to observe the morphologies of the nanoparticles. The TEM was operated at an accelerating voltage of 200 kV. Inductively coupled plasma-mass spectrometer (ICP-MS; Japan Agilent 7500ce) was used to detect the molar ratio of elements, and Fourier Transform Infrared Spectroscopy (FTIR; Perkin-Elmer Instruments LLC, Shelton, CT) to measure the complex compound of thioacetamide with metal ions.

Results and Discussion

SiO_2 nanoparticles

The synthesized SiO_2 nanoparticles were first analyzed by TEM to determine the size distribution and morphology. As illustrated in Figure 1, the average particle size of the silica nanoparticles was 177 ± 26 nm. In this work, silica nanoparticles were used as the model system to study the ZIS coating. Note that the surface properties of GS-NS@SiO_2 is the same as those of SiO_2 nanoparticles. Additionally, our previous work showed that the diameter of SiO_2 core is nearly the same as GS-NS@SiO_2.[17]

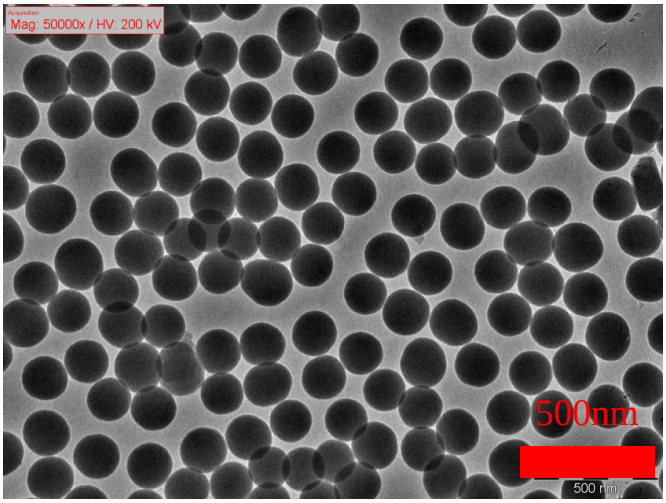

Figure 1. TEM images of silica

DISTRIBUTION A: Approved for public release, distribution unlimited

To modify the surface of SiO_2, 3-mercaptopropyl trimethoxysilane (MPS) was used.[31-35] The morphology of silica without and with modification is shown in Figure 2(a) and (b), respectively. Figure 3 shows the XPS spectra of two samples. For silica with modification, a weak S 2p peak at binding energy = 162-163 eV appeared, belonging –SH function group of the SiO_2@MPS.

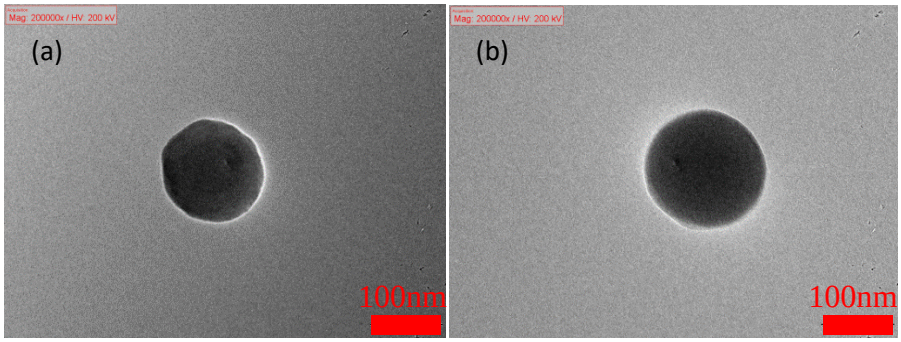

Figure 2. TEM images of (a) SiO_2 (b) SiO_2@MPS

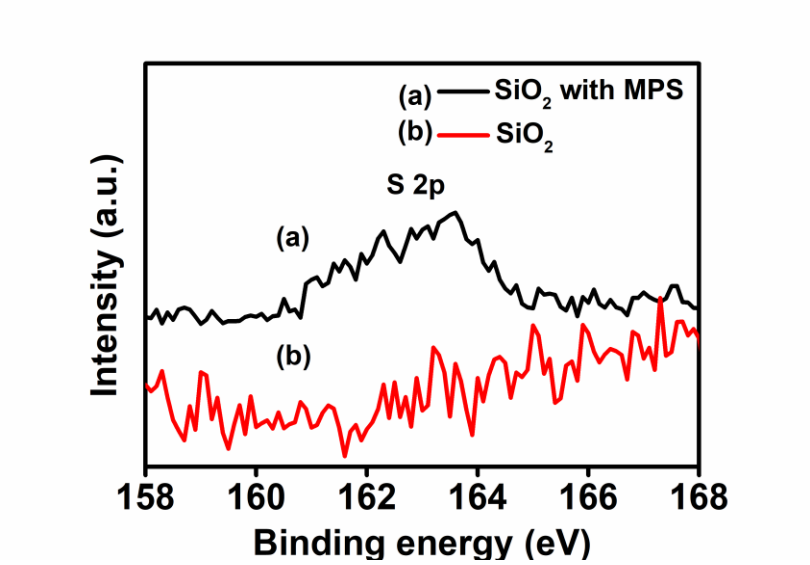

Figure 3. XPS patterns of SiO_2 and SiO_2@MPS.

The ZIS shells were deposited on SiO_2 and SiO_2@MPS in water using low ZIS precursor concentration. Figure 4(a) shows that SiO_2 without modification experiences ZIS aggregation and rough morphology. Instead, SiO_2@MPS with surface modification exhibits homogeneous coverage, as shown in Figure 4(b). The results suggest that the ZIS precursors prefer to absorb on the thiol group. However, if we increase the ZIS precursor concentration, ZIS cannot homogeneously grow onto SiO_2 core, as shown in Figure 5. Throughout this report, SiO_2 nanoparticles with the surface modification were used for the photocatalyst coating. It is important to control the coverage , as well as the crystallinity, for enhanced hydrogen production. In this study, in order to obtain a more efficient photocatalytic catalyst, we use ethanol and HCl to adjust the solution condition to synthesize core–shell SiO_2@MPS@ZIS composites with a better coverage and crystallinity [26-28].

DISTRIBUTION A: Approved for public release, distribution unlimited

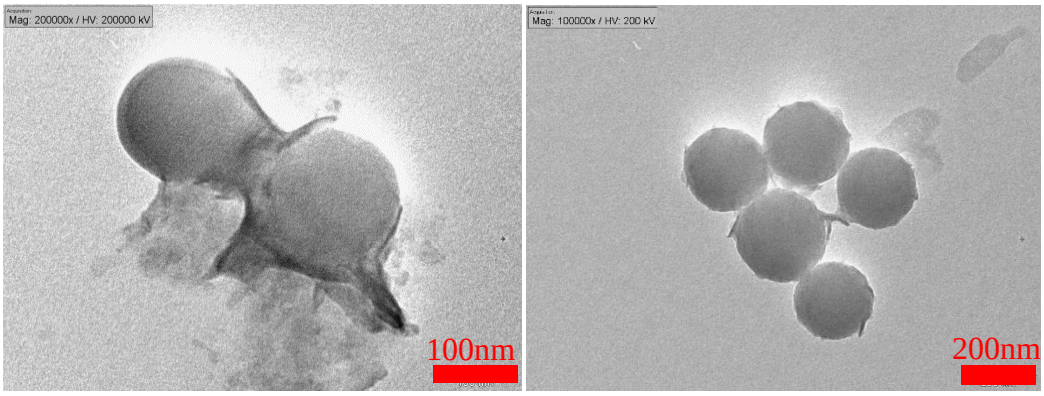

Figure 4. TEM images of (a)SiO_2@ZIS (b)SiO_2@MPS@ZIS with low ZIS concentration synthesized in water.

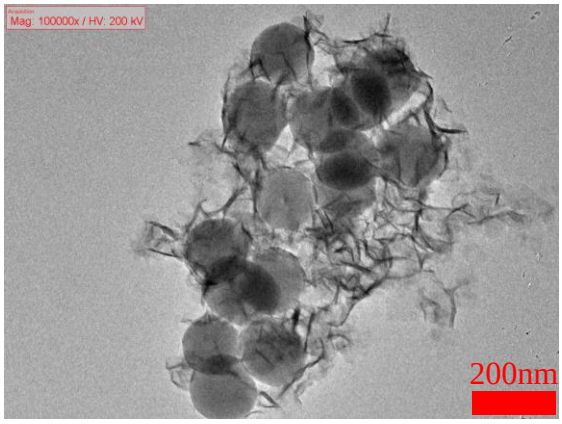

Figure 5. TEM images of SiO_2@MPS@ZIS with normal ZIS concentration synthesized in water.

Core−shell photocatalysts synthesized in water and ethanol.

XRD and TEM were used to detect the crystallinity and coverage of SiO_2@MPS@ZIS synthesized in water and ethanol. 15H denotes SiO_2@MPS@ZIS synthesized in 15 mL water, and 15E denotes particles synthesized in 15 mL ethanol. A better crystalline ZIS core-shell particles synthesized in water were obtained, as judged by the XRD peak intensities, shown in Figure 6. Note that ZIS shell shows the hexagonal phase (JCPDS: 65-2023). On the other hand, Figure 7 indicates that SiO_2@MPS@ZIS synthesized in water appeared aggregate, as compared to the ones synthesized in ethanol. Our goal in this study is to enhance the coverage of ZIS coating onto SiO_2 core. Although SiO_2@ZIS synthesized in ethanol exhibits a good coverage, lower crystallinity would limit the hydrogen production. As a consequence, the pH value was adjusted by adding HCl in ethanol.

DISTRIBUTION A: Approved for public release, distribution unlimited

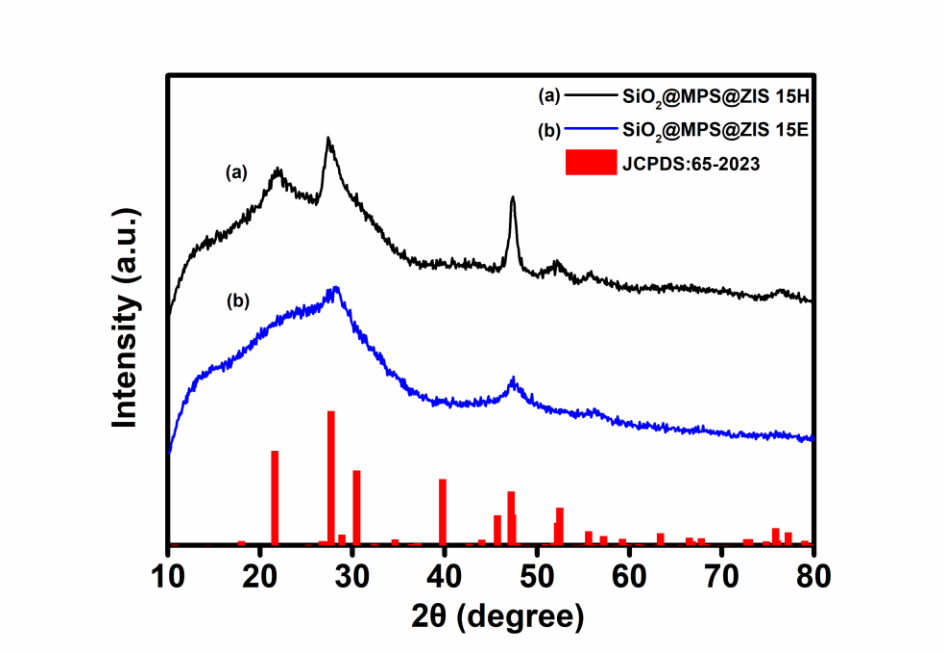

Figure 6. XRD patterns of SiO_2@MPS@ZIS (a)15H (b)15E sample.

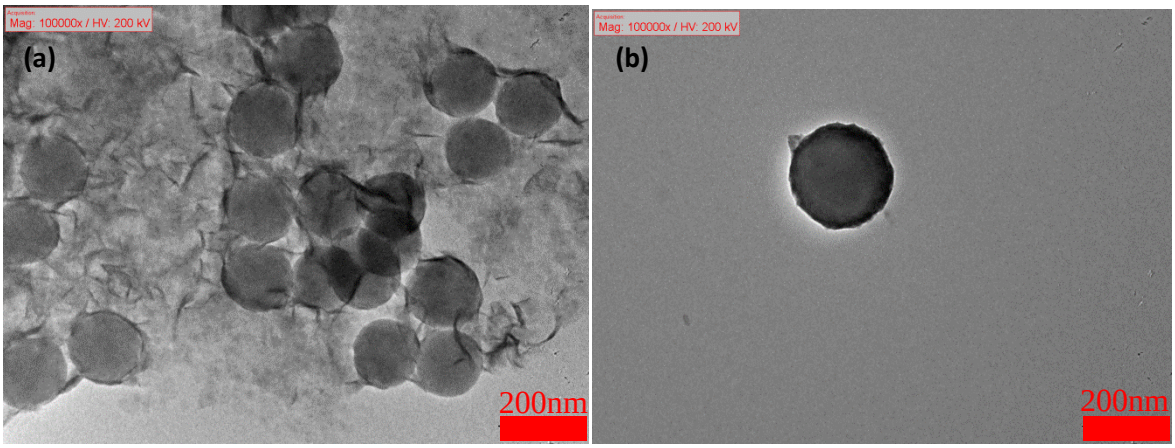

Figure 7. TEM images of SiO_2@MPS@ZIS (a) 15H (b)15E sample.

Core−Shell Photocatalysts synthesized in ethanol with pH control

As mentioned in the previous section, SiO_2@MPS@ZIS core-shell particles exhibits a better surface coverage. In this section, the effects of pH control were investigated. First, HR-TEM and XRD were used to observe the crystal structure, surface morphology, and composition of the core-shell particles synthesized in ethanol with pH = 1. Figure 8(a) shows the TEM image of individual core-shell particle, HR-TEM of lattice analysis, and XRD patterns. Along with Figure 8(b), the line scan and compositional analysis, these data all demonstrated that the materials grown onto SiO_2@MPS is indeed ZIS.

DISTRIBUTION A: Approved for public release, distribution unlimited

The pH of the precursors cannot be precisely controlled by adding HCl in ethanol. Several amounts of HCl were added to study the properties of core-shell particles synthesized in the presence of HCl. The samples were denoted as the following: 15E pH=1.4 is 20 μL HCl; 15E pH=1.2 is 50 μL HCl, and 15E pH=1 is 100μL HCl. When the pH value is lower than 1 in ethanol, ZIS cannot be successfully synthesized. Figure 9 is the XRD patterns of the samples prepared in water and various ethanol solutions. The patterns indicate that the ZIS crystallinity increases with the amount of HCl. The crystal size can be estimated using Scherrer equation. The crystal sizes of these samples was listed in Table 1. It can be found that that SiO_2@MPS@ZIS synthesized in ethanol with lower pH value has a larger crystal size.

Table 1. The mean size of SiO_2@MPS@ZIS d(102) crystalline size (a)15H (b)15E (c)15E pH=1.4 (d)15E pH=1.2 (e)15E pH=1

SiO_2@MPS@ZIS	**15H**	**15E**	**15E pH=1.4**	**15E pH=1.2**	**15E pH=1**
The mean size of d(102) crystalline (nm)	5.05	2.89	3.85	4.63	5.51

DISTRIBUTION A: Approved for public release, distribution unlimited

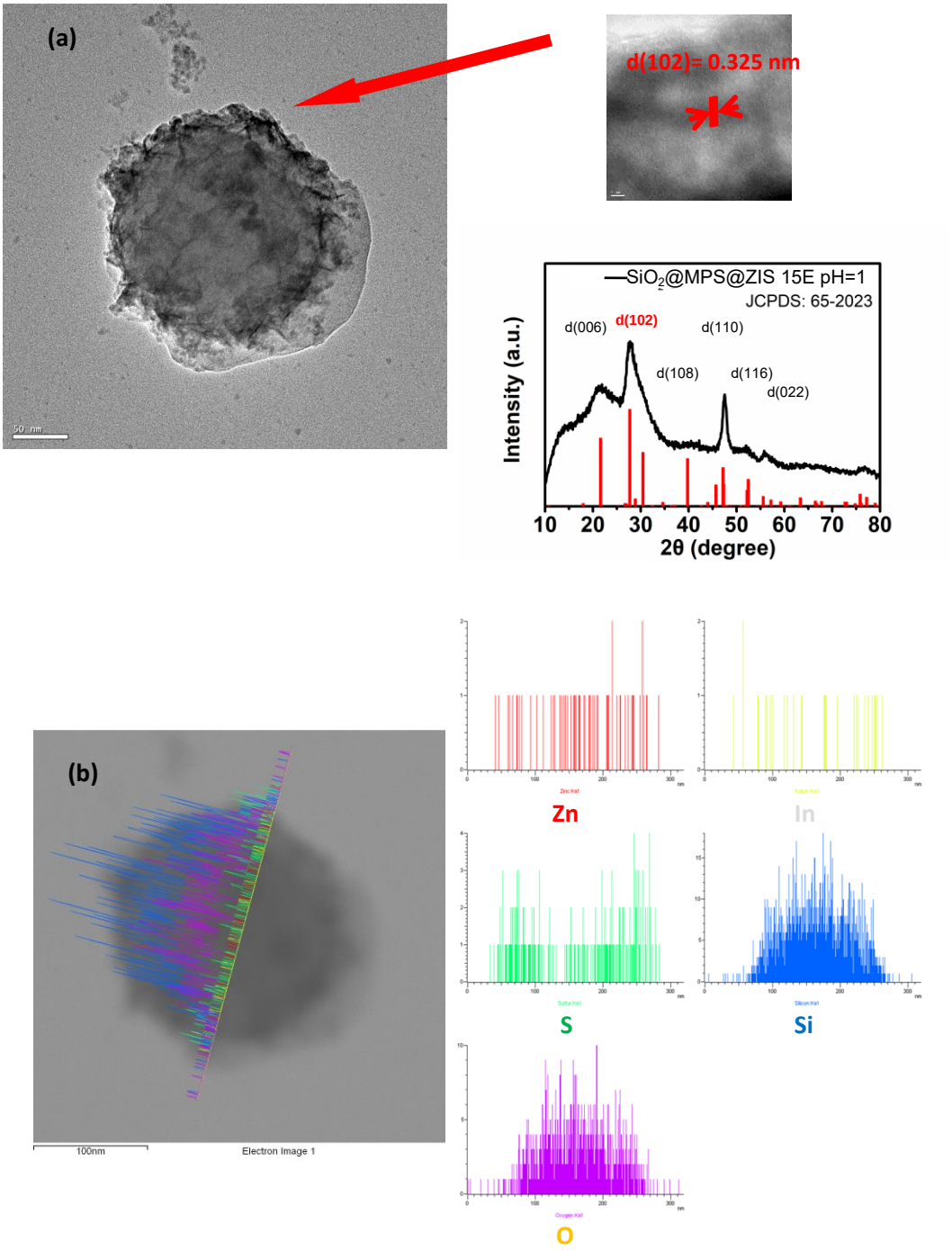

Figure 8. (a)lattice analysis and XRD pattern (b)line scan of SiO_2@MPS@ZIS synthesized in ethanol solution.

DISTRIBUTION A: Approved for public release, distribution unlimited

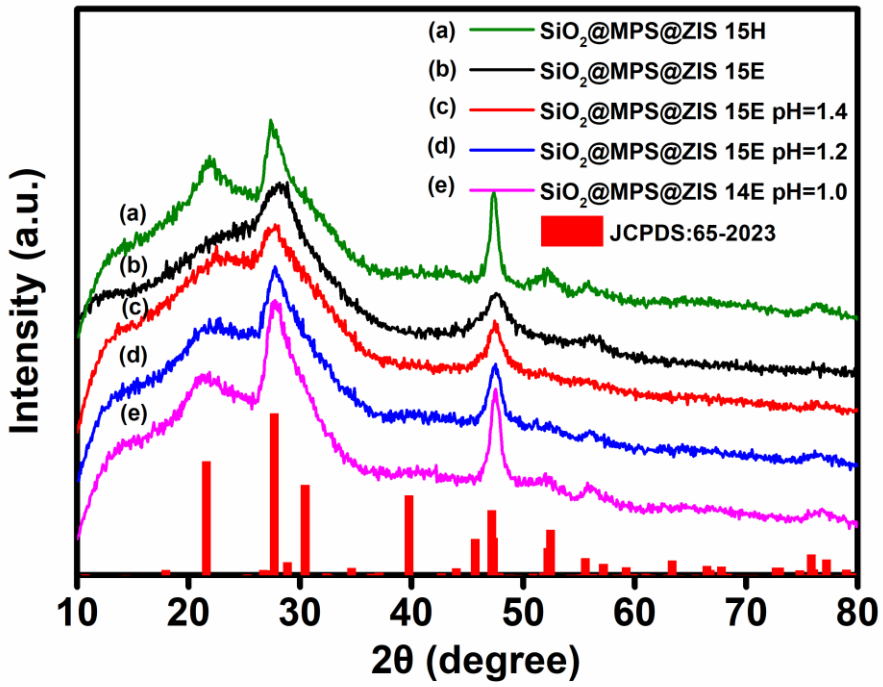

Figure 9. XRD patterns of SiO_2@MPS@ZIS (a)15H (b)15E (c)15E pH=1.4 (d)15E pH=1.2 (e)15E pH=1

Figure 10 shows the TEM images of SiO_2@MPS@ZIS of the samples 15E, 15E pH=1.4, 15E pH=1.2 and 15E pH=1. From these images, ZIS grew homogeneously onto the SiO_2 surfaces. If we closely examine the particles, particles synthesized at lower pH show plate-like surface morphology. Nevertheless, particles synthesized in ethanol with pH control have better coverage than those synthesized in water solution, as shown in Figure 5 and Figure 7 (a). DLS and TEM images were also used to determine the thickness of ZIS shell onto SiO_2. It was found that the thickness varied from 17 nm (pH 1.4) to 27 nm (pH 1). Lower pH precursor solutions lead to thicker ZIS coverage.

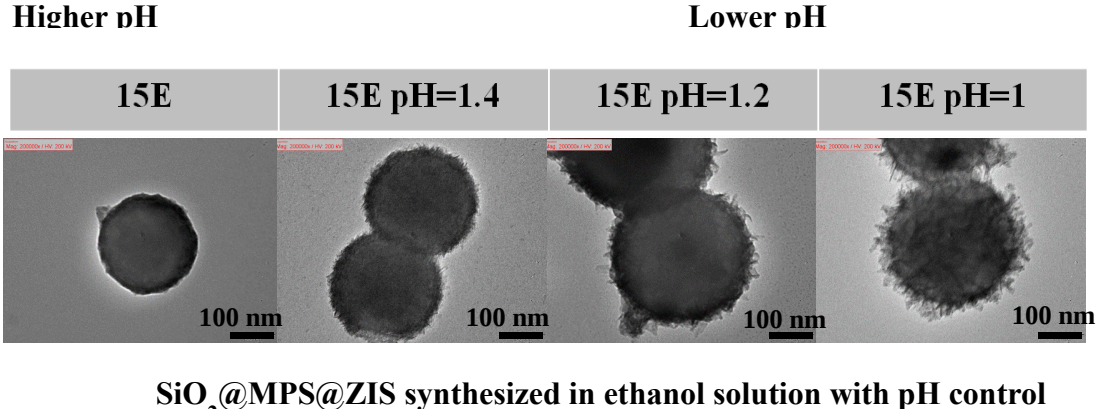

Figure 10. TEM images of SiO_2@MPS@ZIS 15E, 15E pH=1.4, 15E pH=1.2, 15E pH=1

DISTRIBUTION A: Approved for public release, distribution unlimited

FTIR was employed to study the solution chemistry during the ZIS reaction process. Here, ZIS precursors in water and ethanol with SiO_2@MPS were detected by FTIR. The spectra were recorded before precipitation, i.e. the properties of the precursors in these two solvents can be examined. It is observed that, shown in Figure 11, two additional peaks, located at 1320 cm^{-1} 、1645 cm^{-1}, appeared for the ethanol solution. It was reported in the literature that zinc generates complex compound with thioacetamide with the FTIR peak at 1645 cm^{-1}.[36] The peak at 1320 cm^{-1} could be attributed to the complex between indium and thioacetamide. However, the evidence cannot be found in the literature. Nevertheless, the FTIR spectra supports our assertion that in ethanol, the complex can be generated before microwave-assisted hydrothermal process. During hydrothermal process, ZIS grows slowly onto the SiO_2 surface, due to higher viscosity of ethanol.

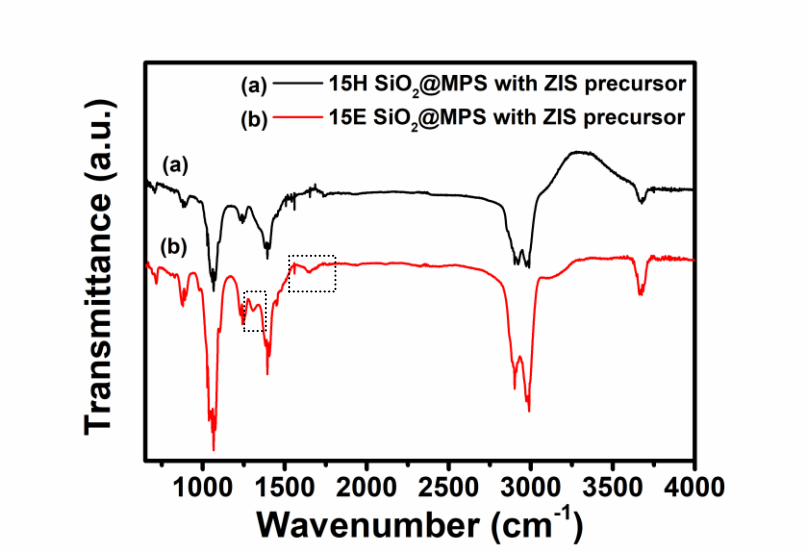

Figure 11. FTIR spectrum of SiO_2@MPS with ZIS precursor in (a) water (b) ethanol solution

Energy band gap is also an important factor for photocatalytic hydrogen production. Figure 12 reveals energy band gap of SiO_2@MPS@ZIS synthesized in water and ethanol with pH control. The absorption of all the samples lie in the visible light region. The values of energy band gap among all samples are quite different, however. 15H is estimated to be 2.14 eV and 15E is 2.48 eV. The energy band gap decreases slowly with a decrease in pH. 15E pH=1.4 is 2.61 eV, 15E pH=1.2 is 2.32 eV and 15E pH=1 is 2.3 eV. ICP-MS was used to determine the compositions, or the molar ratio of zinc, indium and sulfide. As shown in Table 2, the molar ratio of zinc, indium and sulfide for all the samples are different. More importantly, the ratios between ZIS and SiO_2 are different. Note that ZIS grows faster in water. The result again supports our assertion that the higher viscosity of ethanol and complex formed between Zn, In, and thioacetamide reduce the ZIS reaction rate.

DISTRIBUTION A: Approved for public release, distribution unlimited

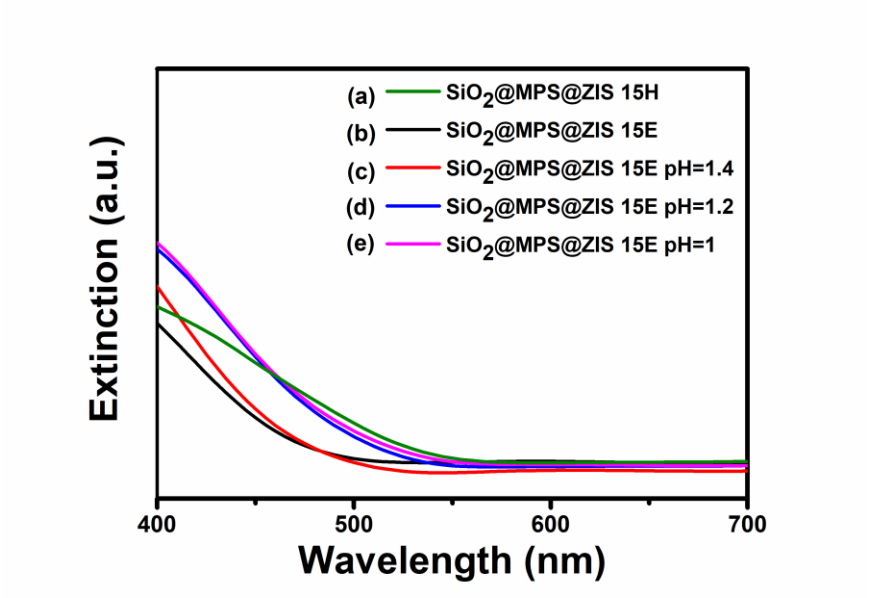

Figure 12. UV spectrums of SiO_2@MPS@ZIS (a)15H (b)15E (c)15E pH=1.4 (d)15E pH=1.2 (e)15E pH=1

Table 2. the ICP-MS measurement data of SiO_2@MPS@ZIS with 50 mg sample.

ICP-MS measurement with 50 mg of sample

Molar ratio	Zn	In	S	ZIS/SiO_2	ZIS/SiO_2@ZIS (g)
SiO_2@MPS@ZIS 15H	1	1.92	3.94	0.45	0.47
SiO_2@MPS@ZIS 15E	1	1.49	3.31	0.54	0.46
SiO_2@MPS@ZIS 15E pH=1	1	3.44	5.90	0.24	0.34

Properties of Photocatalytic H_2 Evolution.

Figure 13 shows the photocatalytic hydrogen evolution rates of the samples synthesized in water and ethanol. The H_2 evolution rate of bare ZIS was also plotted on the same figure. Two major findings can be observed from this figure. 1. ZIS coated onto SiO_2@MPS in water offers larger surface area, leading to a higher hydrogen production rate. 2. Although core-shell particles synthesized in absolute ethanol possess lower hydrogen evolution rate, as compared to those synthesized in water, particles synthesized at lower pH in ethanol exhibit a higher rate. Note also

DISTRIBUTION A: Approved for public release, distribution unlimited

that the hydrogen evolution rate of 15E pH=1 is higher than the sample synthesized in water. Shell thickness of ZIS in ethanol is also shown in Figure 13.

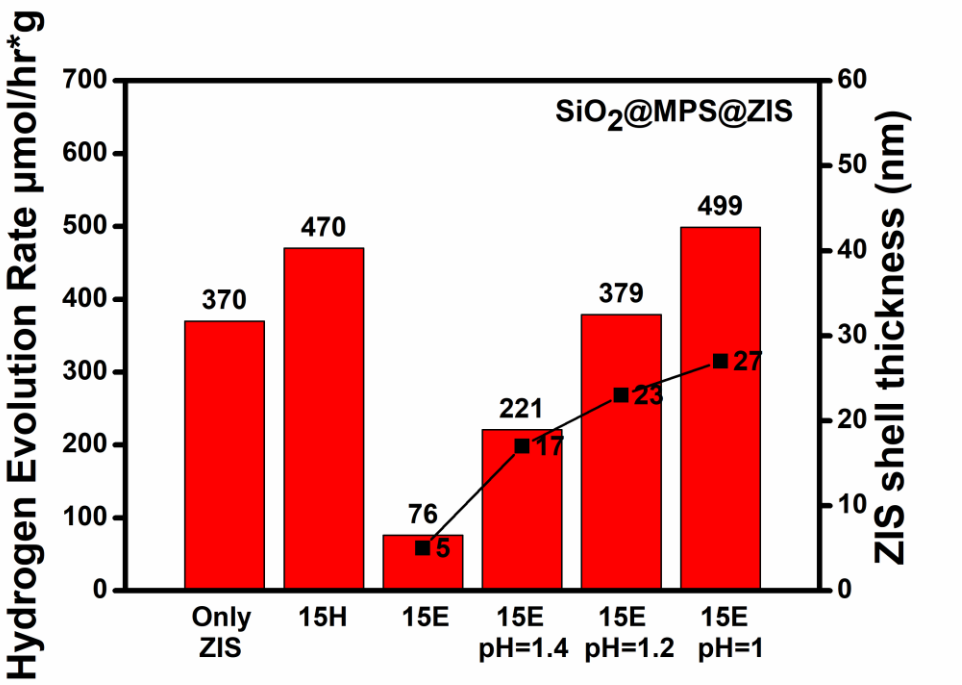

Figure 13. Photocatalytic hydrogen evolution rate of pure ZIS synthesized in water solution and SiO_2@MPS@ZIS 15H, 15E, 15E pH=1.4, 15E pH=1.2, 15E pH=1 with ZIS shell thickness.

We speculate that the hydrogen evolution rate of SiO_2@MPS@ZIS is associated with the crystallinity. To confirm this assertion, the hydrogen production rate was first normalized by the weight of ZIS, as opposed to the total weight of photocatalyst (including SiO_2@MPS). The ratio of ZIS/SiO_2 was estimated using the data in Table 2, and the H_2 evolution rates were calculated accordingly. We could see that SiO_2@MPS@ZIS 15E pH=1 have the least amount of ZIS. Additionally, ZIS/SiO_2 for15H and 15E are nearly the same. The recalculated H_2 production rate per g of ZIS are 1000, 165, and 1467 µmol/h g_{ZIS}, for 15H, 15E, and 15E pH=1, respectively. According to XRD pattern of Figure 9 and hydrogen evolution rate of Figure 13, we could conclude that a better crystalline ZIS shows a better photocatalytic activity.

Next, we explored the possibility to change the thickness of ZIS shell. Here, the concentration of the precursor was changed to control the shell thickness. 2xZIS means double the concentration of ZIS precursor adding to the solution before hydrothermal process, and 3xZIS means three times. Figure 14 shows TEM images of SiO_2@MPS@ZIS 15E pH=1 synthesized in different precursors. It is observed that the thickness of ZIS increases with the concentration of ZIS precursor, while maintaining the crystallinity (Figure 15) and absorption (Figure 16) the same. Hydrogen evolution rate experiment was also carried out, as shown in Figure 17. SiO_2@MPS@ZIS 15E pH=1 has the best hydrogen evolution rate. When the concentration of ZIS precursor increased to three times,

DISTRIBUTION A: Approved for public release, distribution unlimited

the hydrogen evolution rate decreased. It might be due to the over coating of ZIS onto SiO_2@MPS, which might decrease the surface area and absorption of ZIS.

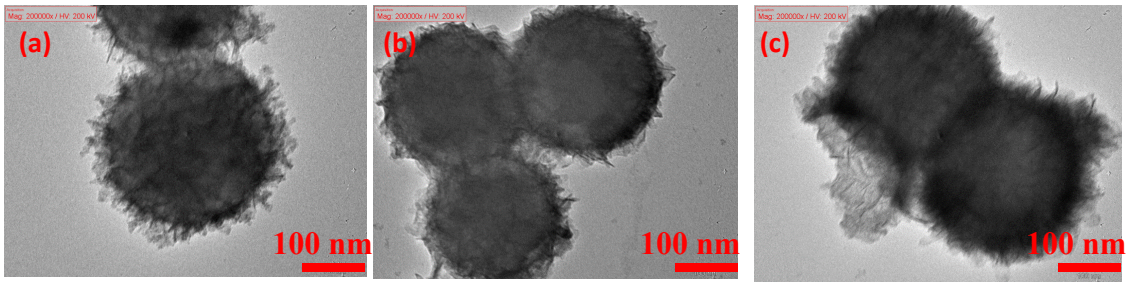

Figure 14. TEM images of SiO_2@MPS@(a)ZIS (b)2xZIS (c)3xZIS 15E pH=1

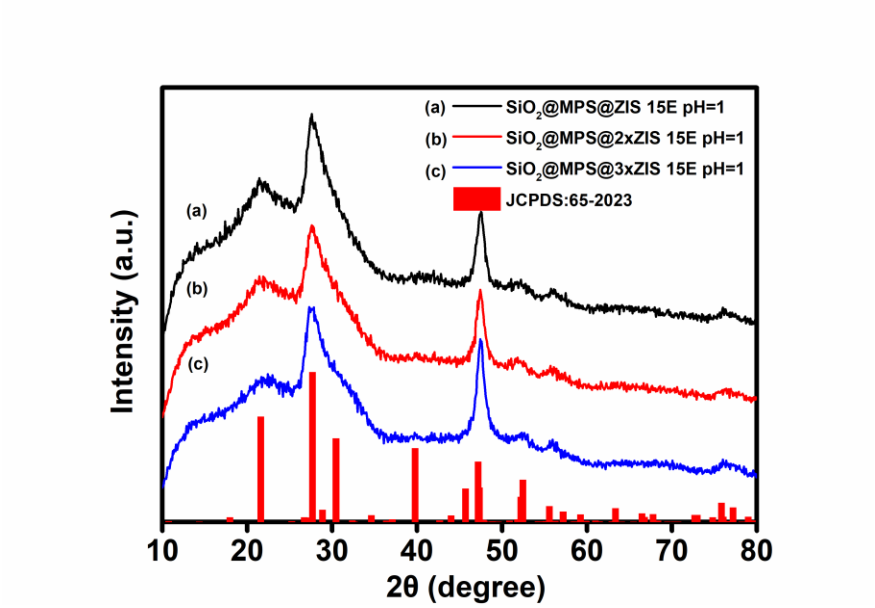

Figure 15. XRD patterns of SiO_2@MPS@ZIS/2xZIS/3xZIS 15E pH=1

DISTRIBUTION A: Approved for public release, distribution unlimited

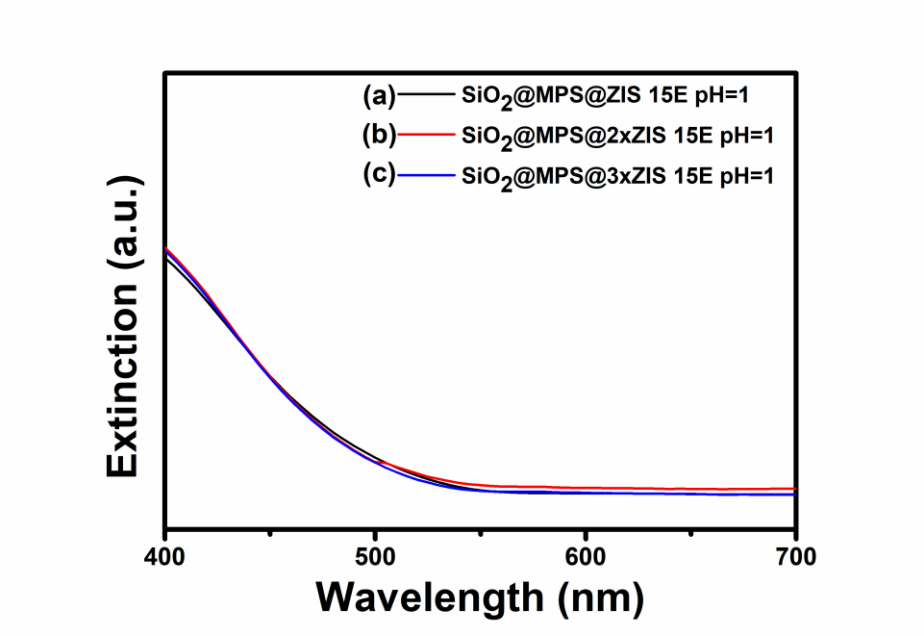

Figure 16. UV spectrums of SiO_2@MPS@ZIS/2xZIS/3xZIS 15E pH=1

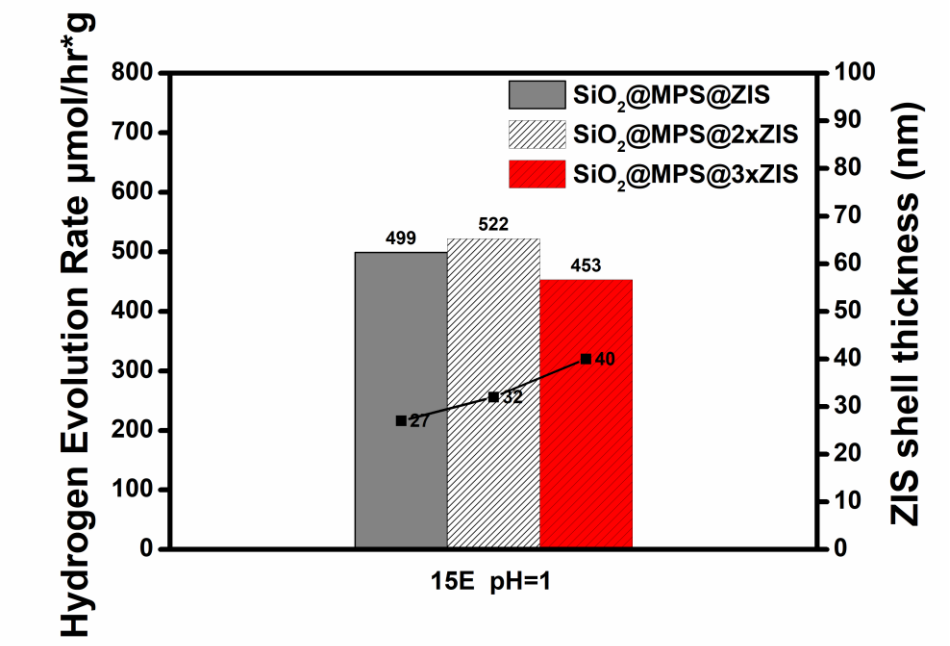

Figure 17. Photocatalytic hydrogen evolution rate and ZIS shell thickness of SiO_2@MPS@ZIS /2xZIS/3xZIS 15E pH=1

The stability of our SiO_2@MPS@ZIS core-shell particles was also evaluated. Figure 18 shows the photocatalytic hydrogen evolution measurements of SiO_2@MPS@ZIS 15E pH=1,

DISTRIBUTION A: Approved for public release, distribution unlimited

repeated for 4 times. It indicates that after four cycles, the SiO_2@MPS@ZIS 15E pH=1 sample still retained its photocatalytic activity.

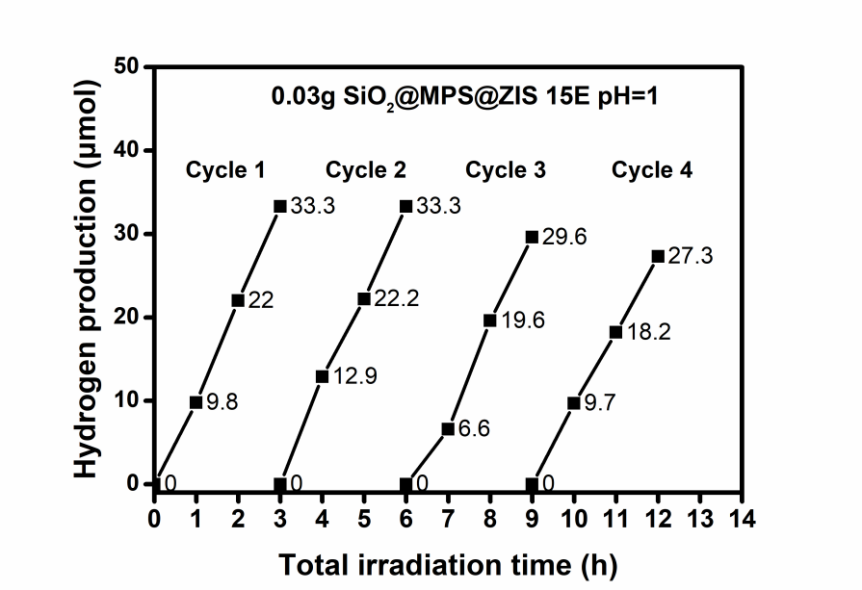

Figure 18. Stability of SiO_2@MPS@ZIS 15E pH=1 with four cycle of hydrogen evolution measurement.

MPS modification on SiO_2 for AIZS coating

In our previous research, MPS modification can increase the coverage of ZIS coating on SiO_2 surface. Here, the same strategy was applied for AIZS synthesis. Figure 19 shows TEM images of the morphologies of SiO_2@AIZS core-shell nanoparticles with (Figure 19(a)) and without (Figure 19(b)) the MPS surface modification. From these figures, AIZS nanoparticles can attach on silica surface more tightly with MPS modification. In contrast, without MPS modification, AIZS nanoparticles just dispersed near silica and generated aggregates (Figure 19(b)).

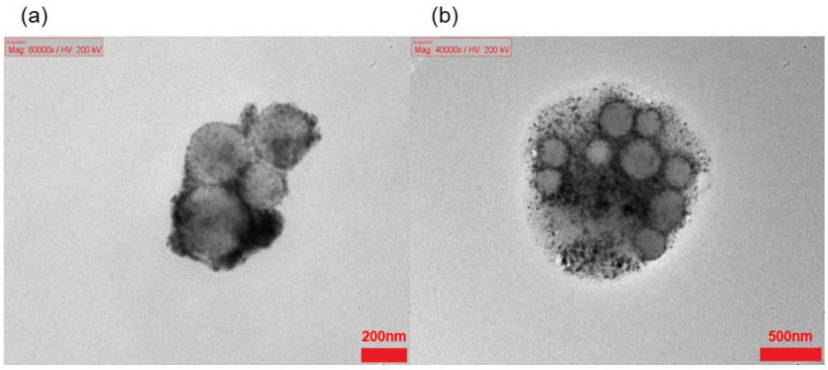

Figure 19. TEM images of AIZS on the silica (a)with (b)without modification

DISTRIBUTION A: Approved for public release, distribution unlimited

Various synthesis temperatures

Figure 20 shows TEM images of SiO_2@MPS@AIZS core-shell particles synthesized at various temperatures, from 200-240 ℃. Our previous research on $ZnIn_2S_4$ indicates that the coverage and crystallinity are critical to the hydrogen generation. Thus, homogeneous AIZS coating on SiO_2 with better crystallinity was sought. From TEM images (Figure 20), AIZS coverage is obviously different at various synthesis temperatures. Based on the TEM images, particles synthesized at 240 ℃ is the best.

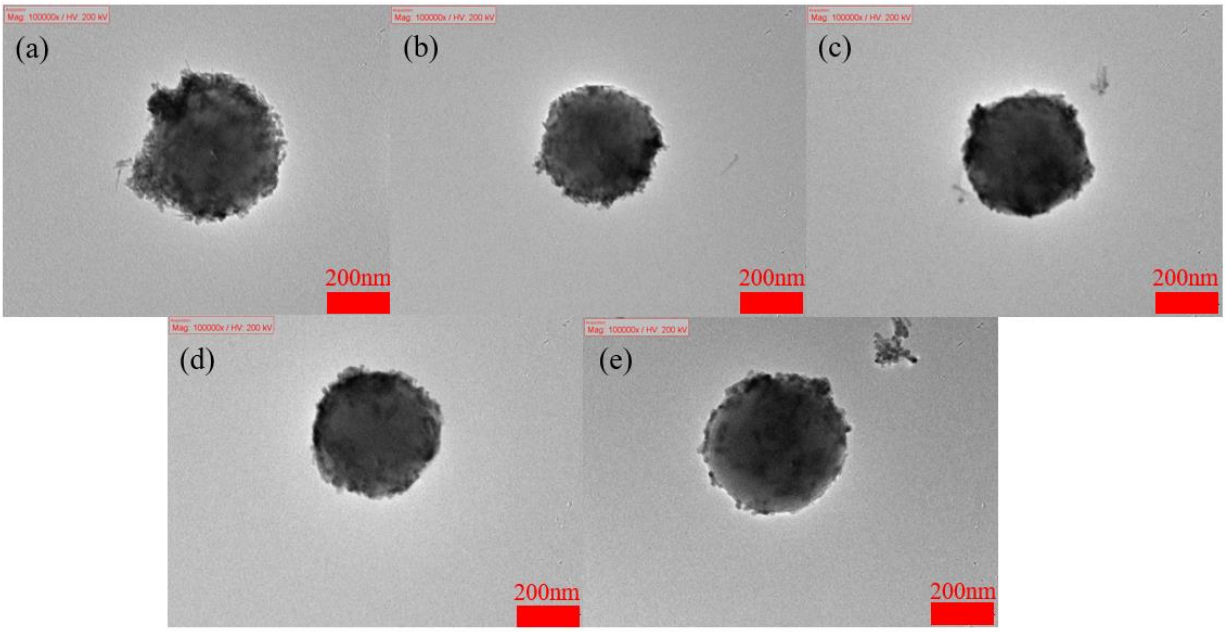

Figure 20. TEM images of different SiO_2@AIZS synthesis temperature (a) 240 ℃ (b) 230 ℃ (c) 220 ℃ (d) 210 ℃ (e) 200 ℃

XRD patterns were recorded and shown in Figure 21. It is evident that the peak intensities increased with synthesis temperature. Nevertheless, two sets of three characteristic peaks between 25-30 degree and 45-55 degree were observed. These six peaks represented the existence of the solid solutions containing $AgInS_2$ and ZnS.

DISTRIBUTION A: Approved for public release, distribution unlimited

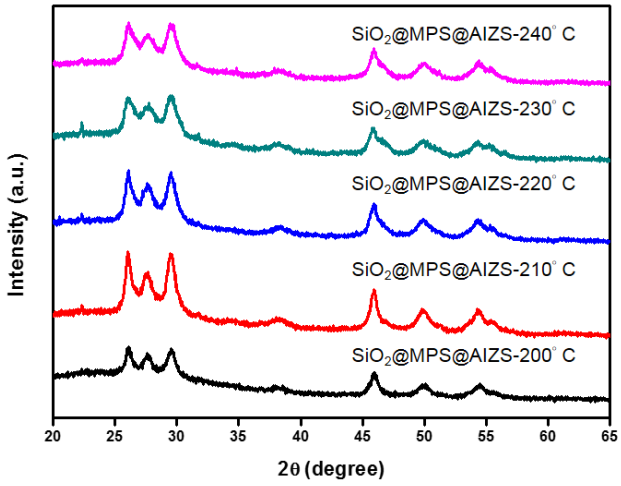

Figure 21. XRD patterns of SiO_2@AIZS synthesized at 200-240 ℃

Hydrogen production using SiO_2@AIZS core-shell particles

Figure 22 shows the photocatalytic hydrogen evolution rate of SiO_2@AIZS synthesized at 200-240 ℃. The highest hydrogen evolution rate, 103 μmol/h*g, was obtained for the sample synthesized at 240 ℃. The hydrogen generation rate of SiO_2@AIZS synthesized at 210-230 ℃ was similar. We suspected that the coverage did not differ much in this temperature interval. The lowest rate occurred for the particles synthesized at 200 ℃, perhaps due to the worst coverage. These results coincide with the TEM images.

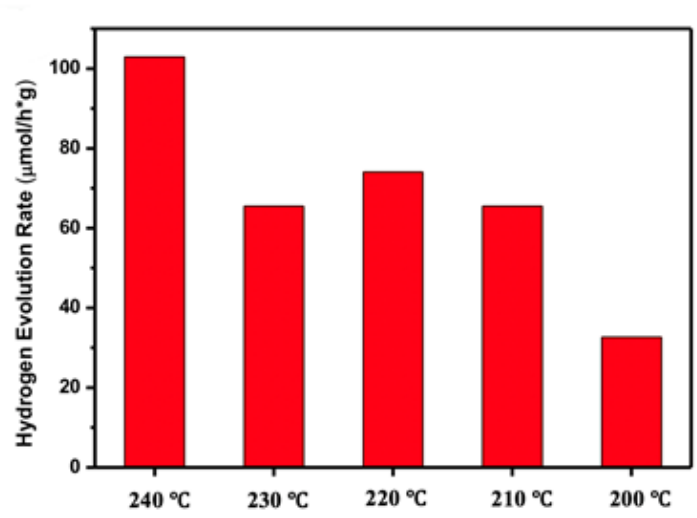

Figure 22. Photocatalytic hydrogen evolution rate of SiO_2@AIZS synthesized at 200-240 ℃

DISTRIBUTION A: Approved for public release, distribution unlimited

List of Publications and Significant Collaborations

Publications

- Lin, P.-C.; Wang, P.-Y.; Li, Y.-Y.; Hua, C. C.; Lee, T.-C., Enhanced Photocatalytic Hydrogen Production over In-rich (Ag-In-Zn)S Particles. *Int. J. Hydrogen Energy* **2013**, *38*, 8254-8262. (AFOSR/AOARD: FA2386-11-1-4081)
- Lee, F.-Y.; Yang, K.-Y.; Wang, Y.-C.; Li, C.-H.; Lee, T. R.; Lee, T.-C., Electrochemical Properties of an $AgInS_2$ Photoanode Prepared Using Ultrasonic-assisted Chemical Bath Deposition. *RSC Adv.* **2014**, *4*, 35215-35223. (AFOSR/AOARD: FA2386-13-1-4032)
- Li, C.-H.; Jamison, A. C.; Rittikulsittichai, S.; Lee, T.-C.; Lee, T. R., In Situ Growth of Hollow Gold–Silver Nanoshells within Porous Silica Offers Tunable Plasmonic Extinctions and Enhanced Colloidal Stability. *ACS Appl. Mater. Interfaces* **2014**, *6*, 19943-19950. (AFOSR/AOARD: FA2386-13-1-4032)
- Zhao, F.; Zeng, J; Arnob, M. M. P.; Sun, P.; Qi, J.; Motwani, P.; Gheewala, M.; Li; Paterson, A.; Strych, U.; Raja, B.; Willson, R. C.; Wolfe, J. C.; Lee, T. R.; Shih, W.-C., Monolithic NPG Nanoparticles with Large Surface Area, Tunable Plasmonics, and High-Density Internal Hot-Spots. *Nanoscale* **2014**, *6*, 8199-8207. (AFOSR/AOARD: FA2386-13-1-4032)
- Li, C.-H.; Li, M.-C.; Jamison, A. C.; Liu, S.-P.; Lee, T. R.; Lee, T.-C., Plasmonically Enhanced Photocatalytic Hydrogen Production from Water: The Critical Role of Tunable Surface Plasmon Resonance from Gold-Silver Nanoshells. *ACS Appl. Mater. Interfaces* **2016**, *8*, 9152-9161. (AFOSR/AOARD: FA2386-14-1-4074 and FA2386-15-1-4101)
- Bryan, W. W.; Jamison, A. C.; Chinwangso, P.; Rittikulsittichai, S.;Lee, T.–C.; Lee, T. R., Preparation of THPC-Generated Silver, Platinum, and Palladium Nanoparticles and Their Use in the Synthesis of Ag, Pt, Pd, and Pt/Ag Nanoshells. *RSC Adv.* **2016**, *6*, 68150-68159. (AFOSR/AOARD: FA2386-15-1-4101)
- Shakiba, A.; Shah, S.; Jamison, A. C.; Rusakova, I.; Lee, T. -C.; Lee. T. R., Silver-Free Gold Nanocages with Near Infrared Extinctions. *ACS Omega*, **2016**, *1*, 456-463. (AFOSR/AOARD FA2386-15-1-4101 and DURIP FA9550-15-1-0374)
- Park, H. H.; Srisombat, L.-o.; Jamison, A. C.; Liu, T.; Marquez, M. D.; Park, H.; Lee, S.; Lee, T.-C.; Lee, T. R., Temperature-Responsive Hydrogel-Coated Gold Nanoshells. *Gels* **2018,** *4*, 28. (AFOSR/AOARD FA2386-16-1-4067 and FA2386-17-1-4028)
- Khantamat, O.; Li, C.-H.; Liu, S.-P.; Liu, T.; Lee, H. J.; Zenasni, O.; Lee, T.-C.; Cai, C.; Lee, T. R., Broadening the Photoresponsive Activity of Anatase TiO2 Particles via Decoration with Partial Gold Shells. *J. Colloid Interface Sci.* **2018,** *513*, 715-725. (AFOSR/AOARD FA2386-16-1-4067)
-
-

Presentations

- T.-C. Lee (2011, Sep). 14th Asian Chemical Congress 2011, Bangkok, Thailand.

DISTRIBUTION A: Approved for public release, distribution unlimited

- T.-C. Lee (2012, May). Invited talk: National Chiao Tung University, Hsinchu, Taiwan.
- T. R. Lee (2012, June). Invited talk: Functional Molecules and Materials Symposium; Walailak University; Nakhon Si Thammarat, Thailand.
- P.-C. Lin and T.-C. Lee (2012, Jul). International Conference of Young Research on Advanced Materials, Singapore.
- T.-C. Lee (2013, Apr.). Invited talk: Chang Gung University, Taoyuan, Taiwan.
- T. R. Lee (2013, July). Invited talk: Indo-US Symposium on Molecular Materials; Bangalore, India.
- Y.-K. Kuo, K.-Y. Yang, and T.-C. Lee (2014, Aug). The 15th IUMRS-International Conference in Asia, Fukuoka, Japan.
- T.-C. Lee and T. R. Lee (2014, Sep). Air Force Research Laboratory, Dayton, Ohio, USA.
- M.-C. Li, P.-C. Lin, T. R. Lee, and T.-C. Lee (2014, Oct). VASSCAA-7, Hsinchu, Taiwan.
- C.-H. Li, T.-C. Lee, and T. R. Lee (2014, Oct). BASF-UH Joint Symposium, Univ. of Houston, Houston, TX, USA.
- T.-C. Lee (2014, Dec.). Invited talk: National Chung Hsing University, Taichung, Taiwan.
- C.-H. Li, T.-C. Lee, and T. R. Lee (2015, Mar). 249th ACS National Meeting & Exposition, Denver, CO, USA.
- T.-C. Lee (2015, Jun.). Invited talk: National Synchrotron Radiation Research Center, Hsinchu, Taiwan.
- T. R. Lee (2015, Oct.). Invited talk: Sogang University; Seoul, South Korea.
- T. R. Lee (2016, May). Keynote Speaker: Research First Look Symposium; Houston, Texas.
- T. R. Lee (2016, May). Invited talk: University of California at Davis; Davis, California.
- T. R. Lee (2016, Jun.). Invited talk: University of California at Merced; Merced, California.

Interaction/Collaboration with AFRL, DoD, Industry

- T.-C. Lee and T. R. Lee (Sep. 10, 2014). Visited United States Air Force Research Laboratory in Dayton, OH.
- T. R. Lee (Aug. 17-18, 2015). Hosted the visit of Dr. Kenneth Caster at the University of Houston, Houston, TX.
- T. R. Lee (Oct. 2, 2015). Met with Dr. Ajit Roy at the University of Houston, Houston, TX.
- T. R. Lee (Oct. 16, 2015). Hosted the visit of Dr. Christopher Bunker, University of Houston, Houston, TX.
- T. R. Lee (Oct. 17, 2015). Hosted Dr. Christopher Bunker and Mr. Donald Minus at the *Houston Energy Day Festival* http://energydayfestival.org/, Houston, TX. *T. R. Lee (Apr. 15, 2016).*
- T. R. Lee (Apr. 15, 2016). *Held preliminary discussions with Dr. Dennis Butcher about starting a new initiative involving the University of Houston, AFOSR, and CONACYT (Mexico's funding agency).*

Team Collaboration Synergy Highlights

DISTRIBUTION A: Approved for public release, distribution unlimited

- Student exchange, Pei-Ying Wang (Jun. 2012) visited UH
- Student exchange, Po-Chang Lin (Jul. 2013) visited UH
- Student exchange, Henry Li (May 2014) visited NCU
- PI visit, T. Randall Lee (May 2014) visited NCU
- PI visit, Tai-Chou Lee (Sep. 2014) visited UH
- Student exchange, Henry Li (Sep. 2015) visited NCU
- Student exchange, Si-Ping Liu (Apr. 2016) visited UH
- PI visit, T. Randall Lee (Oct. 2016) visited NCU
- Student exchange, Yen-Chen Huang (Feb. 2017) visited UH
- Student exchange, Cheng-Yang Wu (Mar. 2018) visited UH

References

1. Gratzel, M., *Photoelectrochemical cells.* Nature, 2001. **414**(6861): p. 338-344.
2. Takata, T., et al., *Fabrication of a Core–Shell-Type Photocatalyst via Photodeposition of Group IV and V Transition Metal Oxyhydroxides: An Effective Surface Modification Method for Overall Water Splitting.* Journal of the American Chemical Society, 2015. **137**(30): p. 9627-9634.
3. Maeda, K. and K. Domen, *Photocatalytic Water Splitting: Recent Progress and Future Challenges.* The Journal of Physical Chemistry Letters, 2010. **1**(18): p. 2655-2661.
4. Kudo, A., *Photocatalyst Materials for Water Splitting.* Catalysis Surveys from Asia, 2003. **7**(1): p. 31-38.
5. Shiga, Y., et al., *A metal sulfide photocatalyst composed of ubiquitous elements for solar hydrogen production.* Chemical Communications, 2016. **52**(47): p. 7470-7473.
6. Tsuji, I., H. Kato, and A. Kudo, *Visible-Light-Induced H2 Evolution from an Aqueous Solution Containing Sulfide and Sulfite over a ZnS–CuInS2–AgInS2 Solid-Solution Photocatalyst.* Angewandte Chemie, 2005. **117**(23): p. 3631-3634.
7. Septina, W., et al., *Photosplitting of Water from Wide-Gap Cu(In,Ga)S2 Thin Films Modified with a CdS Layer and Pt Nanoparticles for a High-Onset-Potential Photocathode.* The Journal of Physical Chemistry C, 2015. **119**(16): p. 8576-8583.
8. Chen, Y.-J.Z.a.F., *Microwave-Assisted Preparation of Inorganic Nanostructures in Liquid Phase.* Chemical Reviews, 2014. **114**(12): p. 6462-6555.
9. Shen, S., et al., *Microwave-assisted hydrothermal synthesis of transition-metal doped ZnIn2S4 and its photocatalytic activity for hydrogen evolution under visible light.* Journal of Power Sources, 2011. **196**(23): p. 10112-10119.
10. Hu, X., et al., *Rapid Mass Production of Hierarchically Porous ZnIn2S4 Submicrospheres via a Microwave-Solvothermal Process.* Crystal Growth & Design, 2007. **7**(12): p. 2444-2448.
11. Tang, X., et al., *Cu-In-Zn-S nanoporous spheres for highly efficient visible-light-driven photocatalytic hydrogen evolution.* New Journal of Chemistry, 2013. **37**(7): p. 1878-1882.
12. Shen, S., et al., *Enhanced Photocatalytic Hydrogen Evolution over Cu-Doped ZnIn2S4 under Visible Light Irradiation.* The Journal of Physical Chemistry C, 2008. **112**(41): p. 16148-16155.

DISTRIBUTION A: Approved for public release, distribution unlimited

13. Hou, J., et al., *Ternary 3D architectures of CdS QDs/graphene/ZnIn2S4 heterostructures for efficient photocatalytic H2 production.* Physical Chemistry Chemical Physics, 2013. **15**(37): p. 15660-15668.
14. Xu, B., et al., *A 1D/2D Helical CdS/ZnIn2S4 Nano-Heterostructure.* Angewandte Chemie International Edition, 2014. **53**(9): p. 2339-2343.
15. Li, Y., et al., *Photocatalytic hydrogen generation in the presence of glucose over ZnS-coated ZnIn2S4 under visible light irradiation.* International Journal of Hydrogen Energy, 2010. **35**(13): p. 7116-7126.
16. Chai, B., et al., *Preparation of a MWCNTs/ZnIn2S4 composite and its enhanced photocatalytic hydrogen production under visible-light irradiation.* Dalton Transactions, 2012. **41**(4): p. 1179-1186.
17. Li, C.-H., et al., *Plasmonically Enhanced Photocatalytic Hydrogen Production from Water: The Critical Role of Tunable Surface Plasmon Resonance from Gold–Silver Nanoshells.* ACS Applied Materials & Interfaces, 2016. **8**(14): p. 9152-9161.
18. Chen, Y., et al., *Hierarchical Core–Shell Carbon Nanofiber@ZnIn2S4 Composites for Enhanced Hydrogen Evolution Performance.* ACS Applied Materials & Interfaces, 2014. **6**(16): p. 13841-13849.
19. Gou, X., et al., *Shape-Controlled Synthesis of Ternary Chalcogenide ZnIn2S4 and CuIn(S,Se)2 Nano-/Microstructures via Facile Solution Route.* Journal of the American Chemical Society, 2006. **128**(22): p. 7222-7229.
20. Shen, S., L. Zhao, and L. Guo, *Crystallite, optical and photocatalytic properties of visible-light-driven ZnIn2S4 photocatalysts synthesized via a surfactant-assisted hydrothermal method.* Materials Research Bulletin, 2009. **44**(1): p. 100-105.
21. Shen, S., L. Zhao, and L. Guo, *Cetyltrimethylammoniumbromide (CTAB)-assisted hydrothermal synthesis of ZnIn2S4 as an efficient visible-light-driven photocatalyst for hydrogen production.* International Journal of Hydrogen Energy, 2008. **33**(17): p. 4501-4510.
22. Jie Chen, C.-L.D., Yuanchang Du,Daming Zhao and Shaohua Shen *Nanogap Engineered Plasmon-Enhancement in Photocatalytic Solar Hydrogen Conversion.* Adv. Mater. Interfaces, 2015. **2**(14): p. 1500280.
23. Varadee Vongsavat, B.M.V., William W. Bryan, Jun-Hyun Kim and T. Randall Lee, *Ultrasmall Hollow Gold Silver Nanoshells with Extinctions Strongly Red-Shifted to the Near-Infrared.* ACS Appl. Mater. Interfaces, 2011. **3**: p. 3616–3624.
24. Cushing, S.K., Li, Jiangtian, Meng, Fanke, Senty, Tess R., Suri, Savan, Zhi, Mingjia, Li, Ming, Bristow, Alan D. and Wu, Nianqiang, *Photocatalytic Activity Enhanced by Plasmonic Resonant Energy Transfer from Metal to Semiconductor.* J. Am. Chem. Soc., 2012. **134**(36): p. 15033-15041.
25. Shen, S., L. Zhao, and L. Guo, *Morphology, structure and photocatalytic performance of ZnIn2S4 synthesized via a solvothermal/hydrothermal route in different solvents.* Journal of Physics and Chemistry of Solids, 2008. **69**(10): p. 2426-2432.
26. Chai, B., et al., *Template-Free Hydrothermal Synthesis of ZnIn2S4 Floriated Microsphere as an Efficient Photocatalyst for H2 Production under Visible-Light Irradiation.* The Journal of Physical Chemistry C, 2011. **115**(13): p. 6149-6155.
27. Li, F., et al., *Hydrothermal synthesis of zinc indium sulfide microspheres with Ag+ doping for enhanced H2 production by photocatalytic water splitting under visible light.* Catalysis Science & Technology, 2014. **4**(4): p. 1144-1150.

DISTRIBUTION A: Approved for public release, distribution unlimited

28. Chen, Z., et al., *Low-Temperature and Template-Free Synthesis of ZnIn2S4 Microspheres.* Inorganic Chemistry, 2008. **47**(21): p. 9766-9772.
29. Stöber, W. and A. Fink, *Controlled growth of monodisperse silica spheres in the micron size range.* J. Colloid Interface Sci., 1968. **26**(2): p. 62-69.
30. Kim, J.-H., H.-W. Chung, and T.R. Lee, *Preparation and Characterization of Palladium Shells with Gold and Silica Cores.* Chemistry of Materials, 2006. **18**(17): p. 4115-4120.
31. Lu, Z., et al., *Direct Assembly of Hydrophobic Nanoparticles to Multifunctional Structures.* Nano Letters, 2011. **11**(8): p. 3404-3412.
32. Zheng, F., N. Zhang, and B. Hu, *Mn(ii) imprinted 3-mercaptopropyltrimethoxysilane (MPTS)-silica coated capillary microextraction on-line hyphenated with inductively coupled plasma mass spectrometry for the determination of trace Mn(ii) in biological samples.* Journal of Analytical Atomic Spectrometry, 2011. **26**(7): p. 1521-1525.
33. Song, J., et al., *Enhanced Antibacterial Activity of Silver/Polyrhodanine-Composite-Decorated Silica Nanoparticles.* ACS Applied Materials & Interfaces, 2013. **5**(22): p. 11563-11568.
34. Kim E. Sapsford, W.R.A., Lorenzo Berti ,Kelly Boeneman Gemmill, Brendan J. Casey,Eunkeu Oh, Michael H. Stewart and Igor L. Medintz, *Functionalizing Nanoparticles with Biological Molecules: Developing Chemistries that Facilitate Nanotechnology.* Chem. Rev., 2013. **113**: p. 1904-2047.
35. Jianbing Wu, L.L., Junbao Xie, Guozhang Ma and Baojun Wang, , *Surface modification of nanosilica with 3-mercaptopropyl trimethoxysilane: Experimental and theoretical study on the surface interaction.* Chem. Phys. Lett., 2014. **591**: p. 227-232.
36. Gosavi, R.K. and C.N.R. Rao, *Infrared absorption spectra of metal complexes of alkylthioureas and some related ligands.* Journal of Inorganic and Nuclear Chemistry, 1967. **29**(8): p. 1937-1945
37. Tatsuya T., et al., *Controlling the Electronic Energy Structure of ZnS-AgInS$_2$ Solid Solution Nanocrystals for Photoluminescence and Photocatalytic Hydrogen Evolution.* The Journal of Physical Chemistry C, 2015. **119**(44): p. 24740-24749.
38. Tsukata T., et al., *Controlling shape Anisotropy of ZnS-AgInS$_2$ Solid Solution Nanoparticles for Improving Photocatalytic Activity.* ACS Applied Materials & Interfaces, 2016 **8**(40): p. 27151-27161
39. Tatsuya K., et al., *Enhanced Photocatalytic Activity of Zn-Ag-In-S Semiconductor Nanocrystals with a Dumbbell-Shaped Heterostructure.* The Journal of Physical Chemistry C, 2018 **122**(25): p. 13705-13715

DISTRIBUTION A: Approved for public release, distribution unlimited